Nanoscale Stratification of Local Optical Fields in Low-Dimensional Atomic Lattices

A. E. Kaplan and S. N. Volkov

Department of Electrical and Computer Engineering, Johns Hopkins University, Baltimore, Maryland 21218, USA

(Received 19 March 2008; published 25 September 2008)

We predict nanoscale field and dipole patterns due to the broken uniformity of a laser-driven local field in 1D and 2D lattices. They may result in size-related resonances and large field enhancement, which in turn can give rise to low-intensity nonlinear optical effects, e.g., optical bistability, even in the ultimate case of a pair of coupled atoms. At certain, ''magic'' numbers and configurations of atoms in a lattice, the system may exhibit the self-induced cancellation of the suppression of a local field.

DOI: 10.1103/PhysRevLett.101.133902 PACS numbers: 42.65.Pc, 85.50.−n

A fundamental fact of the electrodynamics of continuous media is that the microscopic (or *local*) field (LF) acting upon atoms or molecules is generally different from both the applied and average macroscopic fields, because of interparticle interaction. Its best known manifestation is the famous Lorentz–Lorenz relation for dielectrics [1]. A common assumption in local-field theories is that the LF is uniform at distances much shorter than the wavelength of light, λ (amounting to the so-called ''mean-field approximation''). Recent advances in technology allow the fabrication of nanoscale structures where the assumption is no longer valid for sufficiently strong interparticle interaction. One may expect that abandoning the mean-field approximation (similarly, e.g., to the Ising model vs the Curie–Weiss theory of magnetic materials [2]) may bring about significant new phenomena. Two major factors here make a substantial difference compared to the magnetic phenomena: the interaction is driven by an external nonstatic (optical) field, and the system size is small.

We demonstrate in this Letter that the LF varying in space on a scale $\ll \lambda$ may change the entire paradigm of light–matter interaction, and allow for giant LF resonances, ''magic'' configurations, and optical hystereses in 1D and 2D nanostructures. If *local uniformity* is broken by any perturbation, an ordered system of particles may exhibit near-periodic spatial sub-λ patterns (strata) of polarization. They are most pronounced in 1D and 2D dielectric systems of, e.g., atoms, quantum dots, clusters, molecules, etc., that allow to control anisotropy of near-field interaction; if the field propagates normally to the lattice, this also eliminates EM-propagation aspects of the problem. In general, two major modes of the strata transpire: shortwave (SW), with the period up to four atomic spacings, l_a, and long-wave (LW) strata. The strata are standing waves of LF excitations (called here *locsitons* for convenience), having an electrostatic nature and low group velocity; they may be classified as *Frenkel* [3] excitons because of their bound-electron nature.

In the first approximation, the phenomenon is linear in driving field, and the locsitons may be excited within a spectral band much broader than the atomic linewidth. It can be viewed as Rabi broadening of an atomic line by interatomic interactions. The strata are controlled by laser polarization and the strength of atom coupling, Q, *via* atomic density, dipole moments, relaxation, and detuning. Once $|Q| > Q_{\rm cr} = O(1)$, the LF uniformity can be broken by boundaries, impurities, vacancies in the lattice, etc. A striking manifestation of the effect is large field resonances due to locsiton eigenmodes in finite lattices, and—at certain, ''magic'' number of atoms in the lattice—almost complete cancellation of field suppression near atomic resonance; saturation nonlinearity results in hysteresises and optical bistability.

Our model is based on the near-field dipole atomic interactions, with the incident frequency ω being nearly resonant to an atomic transition with a dipole moment d_a at the frequency ω_0. In a standard LF [1] situation, $\lambda \gg l_a$, the field of a dipole in its near vicinity is dominated by a nonradiative, quasistatic component. Using a 2-level model [4] for the transition, we can write LF acting on a dipole at $\mathbf{r}$ [5] as the incident field $\mathbf{E}_{\rm in}$ plus the sum of near-fields from surrounding dipoles at $\mathbf{r}'$ acted upon by respective LF $\mathbf{E}_{\rm L}(\mathbf{r}')$, i.e., $\mathbf{E}_{\rm L}(\mathbf{r}) = \mathbf{E}_{\rm in}(\mathbf{r}) + \mathbf{E}_{\Sigma}(\mathbf{r})$, where

$$\mathbf{E}_{\Sigma} = -\sum_{\rm latt}^{\mathbf{r}'\neq\mathbf{r}} \frac{(Q/4)l_a^3}{|\mathbf{r}'-\mathbf{r}|^3} \frac{3\mathbf{u}[\mathbf{E}_{\rm L}(\mathbf{r}')\cdot\mathbf{u}] - \mathbf{E}_{\rm L}(\mathbf{r}')}{1+|\mathbf{E}_{\rm L}(\mathbf{r}')|^2/E_{\rm sat}^2(1+\delta^2)}, \quad (1)$$

$\mathbf{u}$ is a unit vector along $\mathbf{r}-\mathbf{r}'$, $\delta = T\Delta\omega = T(\omega-\omega_0)$ is a dimensionless laser detuning, $T = 2/\Gamma$ is a transverse relaxation time of the atom with a resonant (homogeneous) linewidth Γ, $Q = 4|d_a|^2 T/\epsilon\hbar l_a^3(\delta+i)$ is a coupling strength, and $E_{\rm sat}^2 = \hbar^2\epsilon/|d_a|^2\tau T$ is saturation intensity; τ is a longitudinal relaxation (or life-) time, and ϵ is a background dielectric constant. Assuming also that $l_a \gg |d_a|/e$, so the wave functions of neighboring atoms do not overlap, we can use a semiclassical approach standard in LF theory of resonant atoms [4]. Large dipole moments in, e.g., *alkali* vapors or CO_2 gas, narrow resonances in solids [6], quantum wells and clusters, may enhance the phenomenon and allow for l_a from a subnanometer to a few tens of nanometers. (Surface plasmons in metal-dielectric composites [7] may involve a long-range dipole interaction not considered here.) The conventional approach to LF, not

used by us here, is to set $\mathbf{E}_{\mathrm{L}}(\mathbf{r}) = \mathbf{E}_{\mathrm{L}}(\mathbf{r}')$ and use an encapsulating sphere around the observation point.

We consider first a basic model of 1D array of atoms lined up along the z axis, spaced by l_a and driven by a linearly polarized laser incident normally to the array [Fig. 1(a)]. Two major configurations transpire here: (a) $\mathbf{E}_{\mathrm{in}} \parallel \hat{e}_z$ ("head-to-tail" lineup), and (b) $\mathbf{E}_{\mathrm{in}} \perp \hat{e}_z$ ("side-by-side" lineup). In both the cases, $\mathbf{E}_{\mathrm{L}} \parallel \mathbf{E}_{\mathrm{in}}$, allowing scalar equations for the field. Using dimensionless notation $\mathcal{E}_n = [E_{\mathrm{L}}(\mathbf{r}_n)/E_{\mathrm{in}}]_{(p)}$, where (p) denotes polarization, $(p) = \parallel, \perp$, we write (1) for both configurations as

$$\mathcal{E}_n - \frac{\delta_R}{2(\delta + i)} \sum_{\mathrm{latt}}^{j \neq n} \frac{\mathcal{E}_j / S}{|j - n|^3} = 1; \qquad 1 \leq n, j \leq N, \quad (2)$$

where $S = \sum_{j=1}^{\infty} j^{-3} \approx 1.202$, $\delta_R = -4SF_{(p)}|d_a|^2 T/\epsilon\hbar l_a^3$, and factor $F_{(p)}$ is as: $F_{\parallel} = 1$ and $F_{\perp} = -1/2$. In near-neighbor (Ising) approximation (NNA), the sum in (2) is replaced by $\mathcal{E}_{n-1} + \mathcal{E}_{n+1}$. In general, a full summation in (2) and NNA produce qualitatively similar results. In 2-atom case the two approaches merge, see below.

For $N \to \infty$, we look for solution of (2) as a sum of a uniform but strongly anisotropic Lorentz LF,

$$\bar{\mathcal{E}} = (\delta + i)/(\delta - \delta_R + i), \quad (3)$$

and oscillating ansatz $\Delta\mathcal{E} \propto \exp(\pm iqn)$, where $q = 2\pi l_a/\Lambda$ is a wave number and Λ is a wavelength, as in, e.g., the phonon theory [3] (except that we have an excitation of bound electrons, not atomic vibrations). At atomic resonance, $\delta = 0$, and strong coupling, $\delta_R^2 \gg 1$, we have Lorentz LF suppressed, $|\bar{\mathcal{E}}_{\mathrm{res}}|^2 \ll 1$, as if it is "pushed out" from the array. $|\bar{\mathcal{E}}|$ peaks, however, at $\delta = \delta_R$,

$$|\bar{\mathcal{E}}_{\mathrm{peak}}|^2 = |\bar{\mathcal{E}}_{\mathrm{res}}|^{-2} = 1 + \delta_R^2. \quad (4)$$

The q numbers are found via dispersion relationship

$$\frac{1}{S} \sum_{n=1}^{\infty} \frac{\cos(nq)}{n^3} = \frac{\delta + i}{\delta_R} \quad (5)$$

(for NNA the left-hand side in (5) is replaced by $\cos q$).

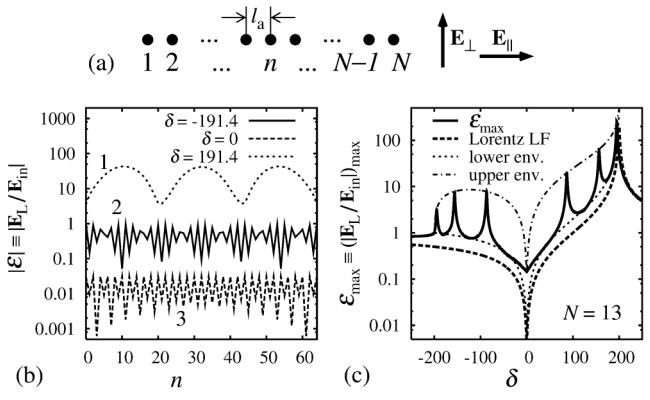

FIG. 1. Local-field $\mathcal{E}$ in 1D array (a) for $\delta_R = 200$: (b) spatial strata of $\mathcal{E}$ vs position n for $N = 65$ and various detunings δ; (c) amplitude resonances of $\mathcal{E}_{\max}$ vs δ (solid line).

Distinct oscillations emerge if $\delta_R^2 > 1$ and $1 > \delta/\delta_R > -3/4$ ($|\delta/\delta_R| < 1$ within NNA), with well-developed patterns at $\delta_R^2 \gg 1$. Lattice dipole–dipole interaction can be gauged by its Rabi frequency (and position of Lorentz resonance), $\Omega_R = \delta_R/T$, or energy band $\sim 2\hbar|\Omega_R| \gg \hbar\Gamma$ (if $\delta_R^2 \gg 1$), similar to that of solid-state [3] and photonic crystals [8]. The limit $1 - \delta/\delta_R \ll 1$ defines LW locsitons,

$$q_{\mathrm{LW}} \approx \sqrt{1 - (\delta/\delta_R)^2}, \qquad \Lambda_{\mathrm{LW}} = 2\pi l_a/q_{\mathrm{LW}}. \quad (6)$$

LW strata [Fig. 1(b), curve 1] emerge near $\delta = \delta_R$; the longest Λ is up to $2\pi l_a \delta_R$. The opposite limit (for NNA it is $1 + \delta/\delta_R \ll 1$) defines SW locsitons, with $q_{\mathrm{SW}} \sim \pi$ and $\Lambda_{\mathrm{SW}}/2 \sim l_a$, the finest grain of locsiton structure. However, a mismatch between $\Lambda_{\mathrm{SW}}/2$ and l_a, whose ratio is in general irrational, results in strong spatial modulation of the SW, giving rise to a *coarse* LW-like structure with the half-period roughly the same as for a LW mode; both of those may be well pronounced [Fig. 1(b), curve 2]. At $\delta \to 0$, the long and short periods converge to $\Lambda = 4l_a$ [Fig. 1 (b), curve 3]. Using phonon analogy, the LW's are counterparts to acoustic, and SW's—to optical phonons.

The LW's may also be viewed as an optical analogy to static ferromagnetic (or ferroelectric) and SW's—to antiferromagnetic states. This analogy is further supported by difference in bistability modes for these two extremes in the case of just two atoms (see below). The excitation at $\delta = 0$ is an example of *hybrid state* (curve 3), with polarization pattern $\uparrow \circ \downarrow \circ \uparrow \cdots$ made possible only by optical nature of dipoles, in contrast to fixed dipoles. A transition from ferromagneticlike to antiferromagneticlike states (through all the intermediate hybrid states) can be attained by simply tuning laser frequency.

A finite array should exhibit size-related resonances. The linear set (2) is readily solved by using numerical matrix solver for $N \gg 1$, as is the case with $\mathbf{E}_{\mathrm{L}}$ in Figs. 1 and 2. It is possible to approximate the solution for finite N as a sum of $\bar{\mathcal{E}}$ ($N = \infty$) and the ansatz $\Delta\mathcal{E} \propto \exp(\pm iqn)$, where both q and amplitude of $\Delta\mathcal{E}$ for the resonances are found from appropriate boundary conditions; we verified it by many numerical simulations. In the NNA case, the half-wavelength $\Lambda_0/2 = (N + 1)l_a$ of fundamental (LW) eigenmode is determined by boundaries as the spacing between LF nodes, $\mathcal{E}_0 = \mathcal{E}_{N+1} = 0$. The kth ($0 < k \leq N$) resonance frequency δ_k is

$$\delta_k = \delta_R \cos(\pi q_k); \qquad q_k = \pi k/(N + 1); \qquad \Lambda_k = \Lambda_0/k. \quad (7)$$

Of these, only the peaks with odd k appear for a symmetric driving profile, and even k—for an antisymmetric one. Figure 1(c) depicts the NNA resonances of maximum amplitude, $\mathcal{E}_{\max}$, for uniform driving, $N = 13$ and $\delta_R = 100$. The lowest amplitude envelope is $\mathcal{E}_{\mathrm{low}}(\delta) \approx 2\bar{\mathcal{E}}$, while the upper envelope of NNA resonant peaks is

$$\mathcal{E}_{\mathrm{up}} \approx \bar{\mathcal{E}}(n_\delta + n_\delta^{-1}), \quad \text{if } n_\delta \leq 1, \quad (8)$$

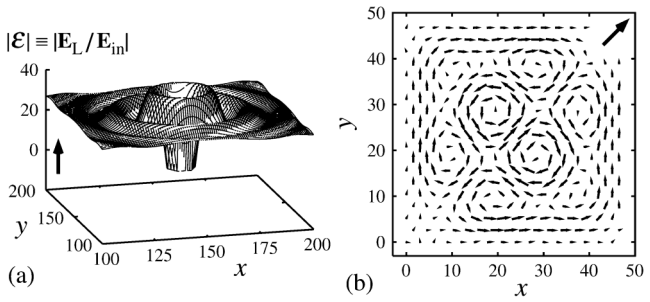

FIG. 2. Local-field $\mathcal{E}$ in a triangular 2D lattice, with driving polarization shown by a big arrow: (a) spatial strata of $\mathcal{E}$ around a 15-point-wide hole at $\delta = 100$ and $\tilde{\delta}_R = 69$; (b) formation of resonant vortices in local-field distribution in the "square"-shaped lattice at $\delta = -1000$ and $\tilde{\delta}_R = 1316.5$ (to avoid crowding, only one of each 9 atoms is shown).

and $= 2\bar{\mathcal{E}}$ otherwise, where $n_\delta = (N+1)/2\sqrt{\delta_R^2 - \delta^2}$. As N increases, the resonances merge, and get damped at $N \sim \delta_R$. However, even then $\mathcal{E}_{\text{low}}$ is still double of the Lorentz field $\bar{\mathcal{E}}$ (3). For $N = 3k-1$ ($k = 1, 2, \ldots$), $\mathcal{E}_{\max}$ dips below $\mathcal{E}_{\text{low}}$ at $\delta = -\delta_R/2$. In this case, $|q| \approx 2\pi/3$, and the NNA SW period is $\Lambda = 3l_a$, so only fine SW structure remains, resulting in antiresonance and strongest inhibition of locsiton.

A fundamental effect of self-induced cancellation of LF suppression emerges near atomic resonance at certain "magic" numbers. If $\delta_R^2 \gg 1$, the Lorentz LF at $\delta = 0$ is very low (4). However, if $N = km_{\text{mag}} + 1$, where $k = 1, 2, \ldots$ and $m_{\text{mag}} = 4$ is a magic number within NNA, the resonant LF suppression gets canceled. The highest cancellation is attained at $N = 5$, with the atoms lining up as $\uparrow \circ \downarrow \circ \uparrow$, where the LF amplitude of odd atoms is maximal, $\mathcal{E}_{\text{mag}} \approx 1/3$, and the enhancement $|\mathcal{E}_{\text{mag}}/\bar{\mathcal{E}}_{\text{res}}|^2 \approx \delta_R^2/9$ could be large; the LF at even atoms almost vanishes. This is due to a standing wave with the nodes at even atoms, hence a mode resonance at the center of atomic line, which manifests itself by enhancement (the resonant peak transpires in $\mathcal{E}_{\text{mag}}/\bar{\mathcal{E}}$ vs δ). The effect holds for the interaction between *all* atoms (2), where it gets a "devilish" streak: $m_{\text{mag}} = 13$. At $\delta = 0$ the first root q_1 of equation $\sum_{n=1}^{\infty} n^{-3}\cos(nq) = 0$ corresponds to q_1/π being almost rational number ($13q_1/6\pi = 1.000\,26\ldots$); hence, the lowest integer of $\Lambda/2$ to match an integer of l_a is $13l_a$, so $N = 14$, with $\mathcal{E}_{\text{mag}} \approx 2/15$.

If the driving wave is spatially limited, a LF can be found beyond that field area; the semantic irony here is that the *local* field phenomenon is due to a *nonlocal* interaction. Locsitons propagate away from their origination point. If $\delta_R^2 > \delta^2 \gg 1$, the group velocity of locsitons is $v_{\text{gr}} = l_a\sqrt{\Omega_R^2 - \Delta\omega^2}$, which could be lower than the speed of sound. This effect can be used for, e.g., developing nanosize delay lines in molecular computers.

2D lattices exhibit even richer stratascape. For a triangular lattice and the polarization of a standing laser wave normal to the plane of lattice, we can see the formation of radial strata around a "hole" in the lattice, Fig. 2(a). More interesting is the configuration with the laser incident normally to the plane of lattice. The simplest approach here is the "nearest-ring" approximation: an atom's environment is viewed as a ring with six atoms evenly "spread" over it. This is a NNA generalization; we can write $Q = \tilde{\delta}_R/(\delta + i)$, where $\tilde{\delta}_R$ is polarization independent and coincides with 1D δ_R at $SF_{(p)} = -1$. Replacing the sum in (1) by integral over the ring, we find the Lorentz LF as isotropic $\bar{\mathbf{E}}_L = \mathbf{E}_{\text{in}}(1 + 3Q/4)^{-1}$. Looking for a full LF again as $\bar{\mathbf{E}}_L$ + "plane wave" locsiton $\propto \exp(\pm i\mathbf{q}\cdot\mathbf{r}/l_a)$ with $\mathbf{q}$ making angle ψ with laser polarization, we obtain an equation for dispersion $q(Q)$, which is a good approximation for LW locsitons:

$$1 + (3Q/4)[J_0(q) - 3J_2(q)\cos(2\psi)] = 0, \qquad (9)$$

where J_n is a Bessel function of the first kind. A more detailed NNA Brillouin zone theory of triangular lattice (which we defer to a later publication) shows that its structure depends on driving polarization relative to the lattice. Well-pronounced patterns in a finite 2D lattice emerge at the "matching" resonances with the same Q in the two orthogonal directions. For an almost "square" lattice, same order LW resonances are attained in both dimensions by picking the right size of the lattice. (Being out of resonance, SW have much lower amplitudes.) Figure 2(b) depicts the vectorial patterns in a nearly square triangular lattice of 48×56 dipoles driven by a laser polarized along the lattice diagonal; a 3rd order resonance is excited in each dimension. We chose here the imaginary field components which are dominant at the resonance; one can see the formation of at least 6 distinct vortices.

Finite 2D lattices may exhibit even greater (vs 1D arrays) magic cancellation of LF suppression (up to 100%), and with a persistent "cabbalistic" streak: within NNA, for $N \leq 15$ the highest effect of fully canceled LF suppression, $\mathcal{E}_{\max} \approx 1.02$, exists only for a six-point star with a central atom ($N = 13$). If $\mathbf{E}_{\text{in}} \parallel \mathbf{u}_K$ in the inner hexagon, the most unaffected by LF are two atoms opposite to each other on the axis of symmetry normal to $\mathbf{u}_K$. Any symmetry violation (e.g., by a foreign atom or molecule attached) will break a sensitive balance of LF and cancellation effect; this can be used, e.g., for biosensing.

Strong driving brings about nonlinear LF effects, e.g., solitons (to be addressed elsewhere). But spectacular effects, such as hystereses and optical bistability, emerge even in steady state. Optical intrinsic bistability for Lorentz LF was predicted in [9] and observed in [10]. However, the possibility for the *nonuniform* multistable SW locsitons is a new development; both of them are best manifested in an extreme example of just two atoms interacting via LF, which is also a most fundamental system to demonstrate self-induced LF nonuniformity.

With $\mathbf{E}_L \parallel \mathbf{E}_{\text{in}}$ being either normal ($\perp$) or parallel ($\parallel$) to the line between atoms, we can use δ_R with $F_\perp$ or $F_\parallel$ in (2)

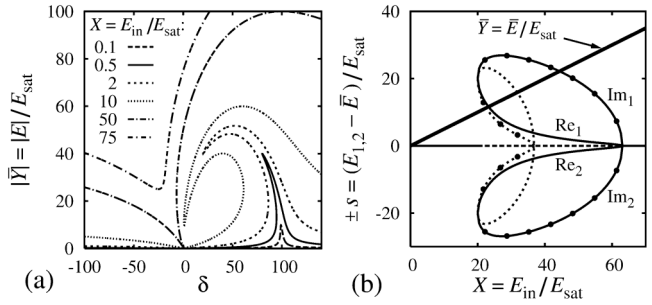

FIG. 3. Multistability of 2-atom nonlinear excitation at $\delta_{R2} = 100$: (a) Lorentz field amplitude $|\bar{Y}|$ vs detuning δ for various driving X; (b) counteroscillating perturbations $\pm s$ of $\bar{Y}$ vs X at $\delta_{R2} + \delta = 10$; thin solid curves show s for stable, and broken curves—for unstable modes. (The dots mark imaginary, and no-dots—real parts of s.)

with $S = 1$. Normalizing both LF amplitudes, $Y_j = E_j/E_{sat}$, $j = 1, 2$, and driving, $X = E_{in}/E_{sat}$, and designating $\delta_{R2} = \delta_R/2 > 0$, we write

$$Y_{3-j} = X + \delta_{R2}(\delta - i)Y_j/(1 + \delta^2 + |Y_j|^2); \qquad j = 1, 2. \tag{10}$$

For a Lorentz LF, it yields a cubic equation for $|\bar{Y}|^2$, readily analyzed. The onset of bistability for $\delta_{R2}^2 \gg 1$ occurs at $\delta \approx \delta_{R2}$, $\delta_{R2} - \delta > \sqrt{3}$, Fig. 3(a), and the threshold driving is $X_{thr}^2 \approx (2/\sqrt{3})^3 \delta_{R2}^{-1} \ll 1$, much below saturation. The 2-atom multistable SW locsiton emerges at the opposite side of the band, at $\delta \approx -\delta_{R2}$. In the limit $X^2 \ll \delta_{R2}^2$, aside from a Lorentz LF, $\bar{Y} \approx X/2$, we find a nonuniform LF solution $Y_{1,2} = \bar{Y} \pm s$, where

$$s = (\sigma/\sqrt{2})(\sqrt{1 \mp R} - i\sqrt{1 \pm R}), \tag{11}$$

$$\sigma = \sqrt{\delta_{R2}(\delta_{R2} + \delta) - 2\bar{Y}^2 \pm \bar{Y}^2 R}, \qquad R = \sqrt{1 - \delta_{R2}^2/\bar{Y}^4}.$$

The solution $\pm s$ allows for interchange $Y_1 \leftrightarrow Y_2$, similarly to the counterwaves bistability in a ring resonator [11]. The necessary conditions for multistability are $\delta_{R2} + \delta > \sqrt{3}$ and $X^2 > 4\delta_{R2}$. Near this threshold the solution is trivalued: bistable (11) and (unstable) Lorentz solution $\bar{Y}$. At $\delta_{R2} + \delta > 2$ it can be five valued [Fig. 3(b)], but only two of them remain stable. The two dipoles then counteroscillate, $\pm s$, akin to two spins, one aligned and another counteraligned with the driving field.

Within solid-state and spin analogies, we note that our findings emphasize phenomena (multiple resonances, magic numbers and shapes, etc.) in relatively small arrays of atoms, in contrast to, e.g., standard approaches to magnetism focused on thermodynamic properties of large systems. Applied to magnetic systems, this new emphasis on nanostructures may reveal similar phenomena.

Nanostrata and locsitons can be observed either via size-related resonances, or x-ray or electron energy loss spectroscopy of the strata. They have promising potential for the molecular computers and nanodevices [12]. The major advantage of locsitons vs electrons in semiconductors or metals is that they are not based on current or charge transfer. This may allow for a drastic reduction of the size limit for elements currently based on metal oxide semiconductors, which on a scale below 10 nm suffer from heat-related problems. The locsiton-based devices could be a complimentary entry into the field as an alternative to emerging technologies such as plasmonics [13] or spintronics [14] by offering both passive (e.g., transmission lines and delays), and active nanoelements for switching and logics. Another application could be biosensing devices, where target-specific receptor molecules form a locsiton-supporting lattice or are attached to its sites; a localized locsiton occurs whenever a target biomolecule attaches to a receptor. Finally, exciting opportunities exist in arrays and lattices with inverse population created by an appropriate (e.g., optical) pumping, which may lead to a laserlike locsiton stimulated emitter (“locster”).

In conclusion, sufficiently dense self-interacting atomic arrays (including atomic pair) and lattices illuminated by a near-resonant radiation can exhibit nanostratification of local-field and atomic polarization, resulting in a host of linear and nonlinear effects, in particular, size-related resonances and field enhancement, “magic”-number cancellation of local-field suppression and optical bistability.

This work is supported by AFOSR.

[1] M. Born and E. Wolf, *Principles of Optics* (Pergamon, Oxford, 1980), Chap. 2, and references therein.
[2] A. Aharoni, *Introduction to the Theory of Ferromagnetism* (Oxford University Press, Oxford, 2001).
[3] C. Kittel, *Introduction to Solid State Physics* (Wiley, New York, 1996).
[4] C. M. Bowden and J. P. Dowling, Phys. Rev. A **47**, 1247 (1993); J. J. Maki, M. S. Malcuit, J. E. Sipe, and R. W. Boyd, Phys. Rev. Lett. **67**, 972 (1991); V. S. Butylkin, A. E. Kaplan, and Y. G. Khronopulo, Sov. Phys. JETP **32**, 501 (1971).
[5] L. D. Landau and E. M. Lifshitz, *The Classical Theory of Fields* (Butterworth, New York, 1980).
[6] D. G. Steel and S. C. Rand, Phys. Rev. Lett. **55**, 2285 (1985).
[7] V. M. Shalaev *et al.*, Opt. Lett. **30**, 3356 (2005); V. A. Markel and A. K. Sarychev, Phys. Rev. B **75**, 085426 (2007).
[8] E. Yablonovitch, Phys. Rev. Lett. **58**, 2059 (1987).
[9] C. M. Bowden and C. C. Sung, Phys. Rev. A **19**, 2392 (1979).
[10] M. P. Hehlen *et al.*, Phys. Rev. Lett. **73**, 1103 (1994).
[11] A. E. Kaplan and P. Meystre, Opt. Commun. **40**, 229 (1982).
[12] J. R. Heath and M. A. Ratner, Phys. Today **56**, No. 5, 43 (2003).
[13] W. A. Murray and W. L. Barnes, Adv. Mater. **19**, 3771 (2007).
[14] I. Žutić, J. Fabian, and S. Das Sarma, Rev. Mod. Phys. **76**, 323 (2004).